High Pressure Research
Vol. 00, No. 00, March 2010, 1–4

arXiv:0912.3616v1 [cond-mat.mes-hall] 18 Dec 2009

RESEARCH ARTICLE

Effect of uniaxial strain on the reflectivity of graphene

F. M. D. Pellegrino[a,b,c], G. G. N. Angilella[a,b,c,d*] and R. Pucci[a,d]

[a]*Dipartimento di Fisica e Astronomia, Università di Catania, Via S. Sofia, 64, I-95123 Catania, Italy*; [b]*Scuola Superiore di Catania, Via S. Nullo, 5/i, I-95123 Catania, Italy*; [c]*INFN, Sez. Catania, I-95123 Catania, Italy*; [d]*CNISM, UdR Catania, I-95123 Catania, Italy*

(*December 18, 2009*)

We evaluate the optical reflectivity for a uniaxially strained graphene single layer between a SiO_2 substrate and air. A tight binding model for the band dispersion of graphene is employed. As a function of the strain modulus and direction, graphene may traverse one of several electronic topological transitions, characterized by a change of topology of its Fermi line. This results in features in the conductivity within the optical range, which might be observable experimentally.

Keywords: graphene; optical reflectivity; uniaxial strain; eletronic topological transition

1. Introduction

Graphene is an atomically thick single layer of carbon atoms in the sp^2 hybridization status, linked to form a honeycomb lattice. This almost unique two-dimensional (2D) structure may be thought of as the building block of three-dimensional (3D) graphite, one-dimensional (1D) nanotubes, and zero-dimensional (0D) fullerenes. The electronic properties of graphene have been known since decades [1]. The band structure consists of two bands, touching at the Fermi level in a linear, cone-like fashion at the so-called Dirac points $\pm\mathbf{K}$. Indeed, the low-energy electronic properties of graphene can be mapped onto those of relativistic massless particles, thus allowing the observation in a solid state system of several effects predicted by quantum electrodynamics [2].

Probably less well known are graphene's equally outstanding mechanical properties. Let alone the very existence of such a 2D crystal, challenging Mermin-Wagner's theorem [2] through the development of relatively small ripples which slightly perturb planarity, graphene achieves the record breaking strength of ~ 40 N/m [3], which nearly equals the theoretical limit, whereas its Young modulus of ~ 1.0 TPa [3] places graphene amongst the hardest materials known. Its electronic, optical, and elastic properties can be strongly modified by uniaxial strain [4] as well as local distortions, such as those caused by local impurities [5]. In particular, recent *ab initio* calculations [6] as well as experiments [7] have demonstrated that graphene single layers can reversibly sustain elastic deformations as large as 20%. In this context, it has been shown that Raman spectroscopy can be used as a sensitive

*Corresponding author. Email: giuseppe.angilella@ct.infn.it

ISSN: 0895-7959 print/ISSN 1477-2299 online
© 2010 Taylor & Francis
DOI: 10.1080/0895795YYxxxxxxxx
http://www.informaworld.com

tool to determine the strain as well as some strain-induced modifications of the electronic and transport properties of graphene [8, 9].

Here, we will be concerned on the effects induced by applied strain on the optical reflectivity of graphene. Based on our previous results for the strain effect on the optical conductivity of graphene [10], we will discuss the frequency dependence of the reflectivity, as a function of strain modulus and direction. We will interpret our results in terms of the proximity to several electronic topological transitions (ETT).

2. Model

The tight-binding Hamiltonian for a honeycomb lattice can be written as

$$H = \sum_{\mathbf{R},\ell} t_\ell a^\dagger(\mathbf{R}) b(\mathbf{R}+\boldsymbol{\delta}_\ell) + \text{H.c.}, \tag{1}$$

where $a^\dagger(\mathbf{R})$ is a creation operator on the position $\mathbf{R}$ of the A sublattice, $b(\mathbf{R}+\boldsymbol{\delta}_\ell)$ is a destruction operator on a nearest neighbor (NN) site $\mathbf{R}+\boldsymbol{\delta}_\ell$, belonging to the B sublattice, and $\boldsymbol{\delta}_\ell$ are the vectors connecting a given site to its NNs, their unstrained values being $\boldsymbol{\delta}_1^{(0)} = a(1,\sqrt{3})/2$, $\boldsymbol{\delta}_2^{(0)} = a(1,-\sqrt{3})/2$, $\boldsymbol{\delta}_3^{(0)} = a(-1,0)$, with $a = 1.42$ Å, the equilibrium C–C distance in a graphene sheet [2]. In Eq. (1), $t_\ell \equiv t(\boldsymbol{\delta}_\ell)$, $\ell = 1,2,3$, is the hopping parameter between two NN sites. In the absence of strain they reduce to a single constant, $t_\ell \equiv t_0$, with $t_0 = -2.8$ eV [11].

In terms of the strain tensor [4]

$$\boldsymbol{\varepsilon} = \varepsilon \begin{pmatrix} \cos^2\theta - \nu\sin^2\theta & (1+\nu)\cos\theta\sin\theta \\ (1+\nu)\cos\theta\sin\theta & \sin^2\theta - \nu\cos^2\theta \end{pmatrix}, \tag{2}$$

the deformed lattice distances are related to the relaxed ones by $\boldsymbol{\delta}_\ell = (\mathbb{I}+\boldsymbol{\varepsilon})\cdot\boldsymbol{\delta}_\ell^{(0)}$. In Eq. (2), θ denotes the angle along which the strain is applied, with respect to the x axis in the lattice coordinate system, ε is the strain modulus, and $\nu = 0.14$ is Poisson's ratio, as determined from *ab initio* calculations for graphene [12], to be compared with the known experimental value $\nu = 0.165$ for graphite [13]. The special values $\theta = 0$ and $\theta = \pi/6$ refer to strain along the armchair and zig zag directions, respectively.

The band structure derived from Eq. (1), also including overlap between NNs [5], is characterized by two bands $E_{\mathbf{k}\lambda}$ ($\lambda = 1,2$) touching cone-like at the Fermi level at the Dirac points $\pm\mathbf{k}_D$ [10]. While at zero strain these coincide with the high symmetry points $\pm\mathbf{K}$ at the vertices of the hexagonal first Brillouin zone (1BZ) of graphene, their positions move away from $\pm\mathbf{K}$ with increasing strain. Depending on the strain modulus and strength, with increasing strain they may eventually merge into the midpoints of one of the sides of the 1BZ. In that case, the cone approximation breaks down, and a finite gap opens at the Fermi level [10]. For intermediate strains, the constant energy contours of $E_{\mathbf{k}\lambda}$ can be grouped according to their topology, and are divided by three separatrix lines [10]. This corresponds to having three distinct electronic topological transitions (ETT) [14, 15, 16], which are here tuned by uniaxial strain, as has been suggested to be the case in other quasi-2D materials, such as the cuprates [17, 18] and the Bechgaard salts [19]. Correspondingly, while the density of states (DOS) is characterized by a linear behaviour close to the Fermi level, because of the linearity in $E_{\mathbf{k}\lambda}$ at $\mathbf{k} = \pm\mathbf{k}_D$, a detailed analysis beyond the cone approximation reveals the presence

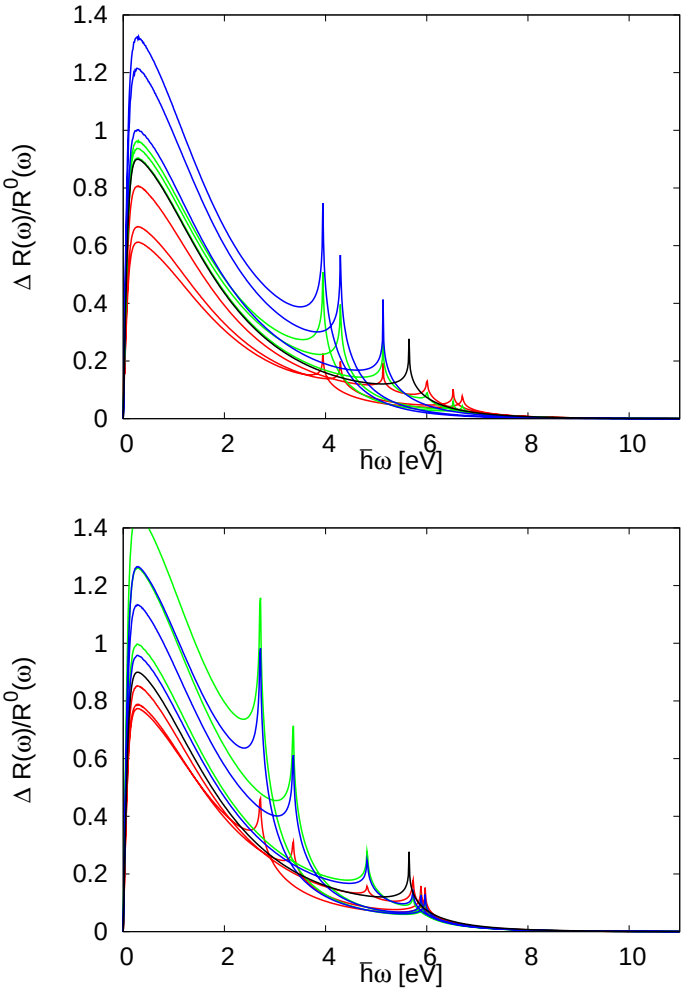

Figure 1. (Color online) Relative reflectivity $\Delta R(\omega)/R^0(\omega)$ as a function of frequency ω for a graphene monolayer between SiO_2 and air. Top panel shows cases with strain applied along the $\theta = 0$ (armchair) direction, while bottom panel shows cases with $\theta = \pi/6$ (zig zag). Different colors refer to a different polarization of the electric field: $\phi = 0$ (red), $\phi = \pi/4$ (green), $\phi = \pi/2$ (blue). Black solid line refers to the unstrained case. Within each group of lines, modulus of applied strain increases as $\varepsilon = 0.025$, 0.075, 0.1 (bottom to top).

of logarithmic singularities in the DOS at higher energies, that may be connected with the proximity to the ETTs [10]. This behaviour is reproduced in the frequency dependence of the longitudinal optical conductivity $\sigma(\omega)$, which has been studied at increasing strain modulus and different strain directions [10].

3. Results and conclusions

We consider light scattering across two media, with refraction index $n_i(\omega)$ $(i = 1, 2)$, separated by a graphene monolayer. In the case of normal incidence, the reflectivity of such a system can be written as [20]

$$R(\omega) = \left(\frac{n_1(\omega) + \frac{\sigma(\omega)}{\epsilon_0 c} - n_2(\omega)}{n_1(\omega) + \frac{\sigma(\omega)}{\epsilon_0 c} + n_2(\omega)} \right)^2 . \tag{3}$$

Assuming air on top of graphene, we have $n_2(\omega) = 1$, whereas we can model the frequency dependence of the refraction index of the substrate through Cauchy's

law, as $n_1(\omega) = n_1(0) + \omega^2/\omega_b^2$. In the case of SiO_2, from a fit of data in Ref. [21], we find $n_1(0) = 1.448$ and $E_b = \hbar\omega_b = 3.305$ eV. We evaluate $\sigma(\omega)$ as in Ref. [10].

Fig. 1 then shows our results for the relative reflectivity $\Delta R(\omega)/R^0(\omega) \equiv [R(\omega) - R^0(\omega)]/R^0(\omega)$, where $R(\omega)$ is the reflectivity of a single graphene monolayer with applied strain, between SiO_2 and air, Eq. (3), and $R^0(\omega)$ refers to the case without the insertion of a graphene layer. We specifically consider applied strain along the armchair ($\theta = 0$) and zig zag ($\theta = \pi/6$) directions. Different colors refer to different polarization angles of the electric field (though always with normal incidence). In all cases, the black solid line refers to the case without strain, where the reflectivity does not depend on the electric field polarization angle.

While at large frequencies the reflectivity invariably tends to the case without graphene, differences are to be seen in the low-frequency range. In particular, the presence of logarithmic spikes can be associated with the proximity to the electronic topological transitions referred to above, their actual position depending on the strain modulus ε, as well as on the relative orientation of strain θ and electric field polarization angle ϕ.

References

[1] P.R. Wallace, *The Band Theory of Graphite*, Phys. Rev. 71 (1947), p. 622.
[2] A.H. Castro Neto, F. Guinea, N.M.R. Peres, K.S. Novoselov, and A.K. Geim, *The electronic properties of graphene*, Rev. Mod. Phys. 81 (2009), p. 000109.
[3] C. Lee, X. Wei, J.W. Kysar, and J. Hone, *Measurement of the Elastic Properties and Intrinsic Strength of Monolayer Graphene*, Science 321 (2008), p. 385.
[4] V.M. Pereira, A.H. Castro Neto, and N.M.R. Peres, *Tight-binding approach to uniaxial strain in graphene*, Phys. Rev. B 80 (2009), p. 045401 preprint `arXiv:0811.4396`.
[5] F.M.D. Pellegrino, G.G.N. Angilella, and R. Pucci, *Effect of impurities in high-symmetry lattice positions on the local density of states and conductivity of graphene*, Phys. Rev. B 80 (2009), p. 094203 preprint `arXiv.org/0909.1903`.
[6] F. Liu, P. Ming, and J. Li, *Ab initio calculation of ideal strength and phonon instability of graphene under tension*, Phys. Rev. B 76 (2007), p. 064120.
[7] K.S. Kim, Y. Zhao, H. Jang, S.Y. Lee, J.M. Kim, K.S. Kim, J.H. Ahn, P. Kim, J. Choi, and B.H. Hong, *Large-scale pattern growth of graphene films for stretchable transparent electrodes*, Nature 457 (2009), p. 706.
[8] Z.H. Ni, T. Yu, Y.H. Lu, Y.Y. Wang, Y.P. Feng, and Z.X. Shen, *Uniaxial Strain on Graphene: Raman Spectroscopy Study and Band-Gap Opening*, ACS Nano 2 (2008), p. 2301.
[9] T.M.G. Mohiuddin et al., *Uniaxial strain in graphene by Raman spectroscopy: G peak splitting, Grüneisen parameters, and sample orientation*, Phys. Rev. B 79 (2009), p. 205433.
[10] F.M.D. Pellegrino, G.G.N. Angilella, and R. Pucci, *Strain effect on the optical conductivity of graphene*, Phys. Rev. B (accepted) ... (2009), p. ... preprint `arXiv.org/0912.3614`.
[11] S. Reich, J. Maultzsch, C. Thomsen, and P. Ordejón, *Tight-binding description of graphene*, Phys. Rev. B 66 (2002), p. 035412.
[12] M. Farjam and H. Rafii-Tabar, *Comment on "Band structure engineering of graphene by strain: First-principles calculations"*, Phys. Rev. B ... (2009), p. ... (submitted for publication; preprint `arXiv:0903.1702`).
[13] O.L. Blakslee, D.G. Proctor, E.J. Seldin, G.B. Spence, and T. Weng, *Elastic Constants of Compression-Annealed Pyrolytic Graphite*, J. Appl. Phys. 41 (1970), p. 3373.
[14] I.M. Lifshitz, *Anomalies of electron characteristics of a metal in the high pressure region*, Sov. Phys. JETP 11 (1960), p. 1130 [Zh. Eksp. Teor. Fiz. **38**, 1569 (1960)].
[15] Ya. M. Blanter, M.I. Kaganov, A.V. Pantsulaya, and A.A. Varlamov, *The theory of electronic topological transitions*, Phys. Rep. 245 (1994), p. 159.
[16] A.A. Varlamov, G. Balestrino, E. Milani, and D.V. Livanov, *The role of density of states fluctuations in the normal state properties of high-T_c superconductors*, Adv. Phys. 48 (1999), p. 655.
[17] G.G.N. Angilella, E. Piegari, and A.A. Varlamov, *Effects of an electronic topological transition for anisotropic low-dimensional superconductors*, Phys. Rev. B 66 (2002), p. 014501.
[18] G.G.N. Angilella, G. Balestrino, P. Cermelli, P. Podio-Guidugli, and A.A. Varlamov, *Effects of strain-induced electronic topological transitions on the superconducting properties of $La_{2-x}Sr_xCuO_4$ thin films*, Eur. Phys. J. B 26 (2002), p. 67.
[19] G.G.N. Angilella, E. Piegari, R. Pucci, and A.A. Varlamov, *Anisotropic low-dimensional superconductors close to an electronic topological transition*, H.D. Hochheimer, B. Kuchta, P.K. Dorhout and J.L. Yarger, eds., , Vol. 48 of *NATO Science Series* Kluwer, Dordrecht, 2001.
[20] T. Stauber, N.M.R. Peres, and A.K. Geim, *Optical conductivity of graphene in the visible region of the spectrum*, Phys. Rev. B 78 (2008), p. 085432.
[21] I. Jung, M. Pelton, R. Piner, D.A. Dikin, S. Stankovich, S. Watcharotone, M. Hausner, and R.S. Ruoff, *Simple Approach for High-Contrast Optical Imaging and Characterization of Graphene-Based Sheets*, Nano Lett. 7 (2007), p. 3569.

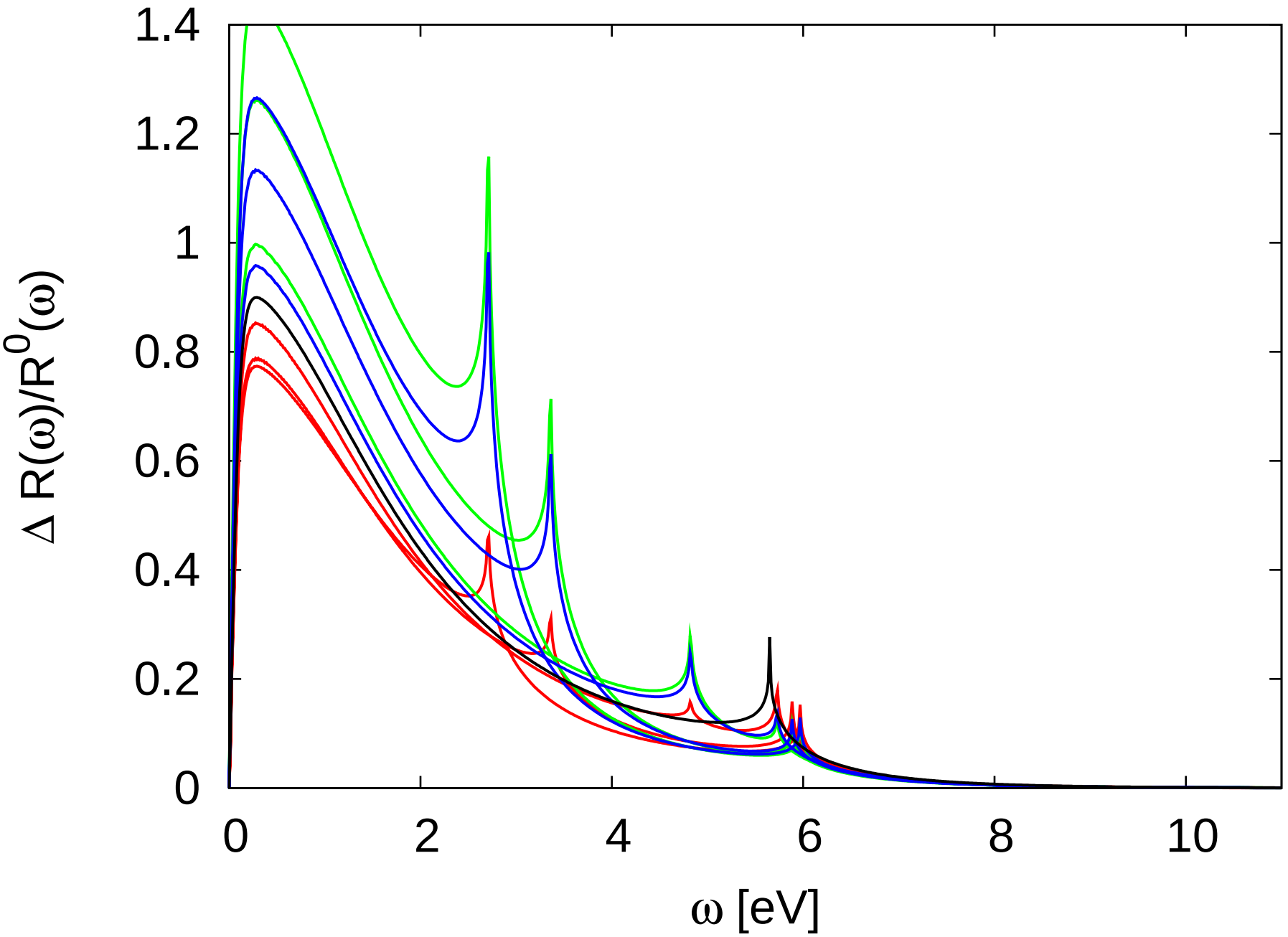
1.4
1.2
1
0.8
0.6
0.4
0.2
0
0
2
4
6
8
10
Δ R(ω)/R0(ω)
ω [eV]

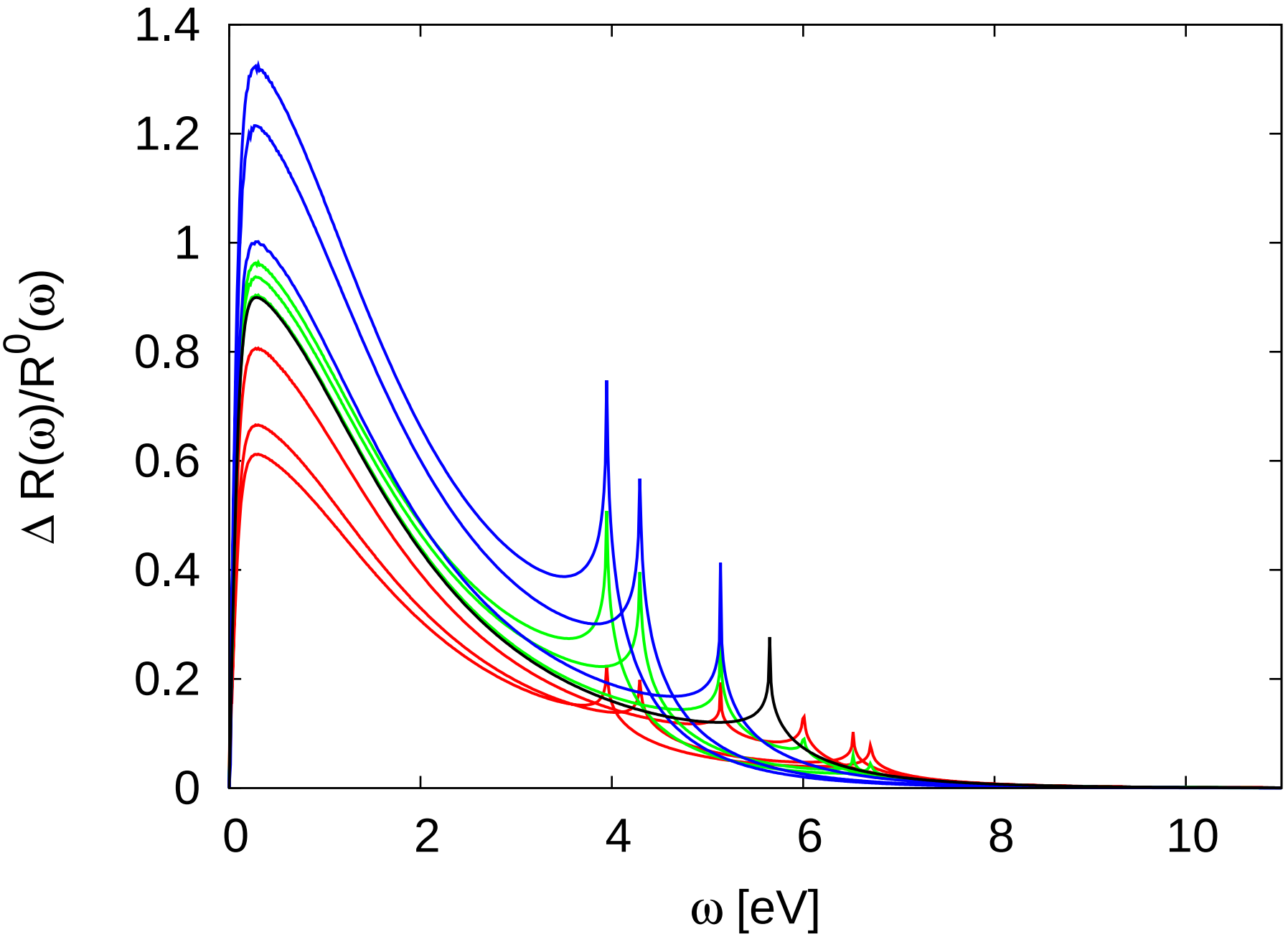
1.4
1.2
1
0.8
0.6
0.4
0.2
0
0
2
4
6
8
10
Δ R(ω)/R0(ω)
ω [eV]